第 22 卷 第 3 期
2005 年 6 月

量 子 电 子 学 报
CHINESE JOURNAL OF QUANTUM ELECTRONICS

Vol.22 No.3
Jun. 2005

文章编号： 1007-5461(2005)03-0377-05

Study on UV laser generated by SRS of CH_4 for NO_2 DIAL measurements

XU Ben[1,2], *YUE Gu-ming*[1], *WU Yong-hua*[1],
ZHOU Jun[1], *ZHANG Yin-chao*[1], *HU Huan-ling*[1]

(1 National Key Laboratory of Atmospheric Optics, Anhui Institute of Optics and Fine Mechanics, Chinese Academy of Sciences, Hefei 230031, China ;
2 Optoelectronics Technology Institute, China Institute of Metrology, Hangzhou 310018, China)

Abstract: The first Stokes radiation (S1, 395.6 nm) of SRS of CH_4, pumped by a pulsed Nd:YAG laser at 355nm, is used as λ_{on} of NO_2-DIAL. A numerical study is done, aiming to explain qualitatively the practically important physical behavior of the configurations. And a series of experiments are reported here on the generation of Stokes orders generated in CH_4. By adjusting pumping laser energy, beam quality and the pressure of gas, the relationship between them and the energy conversion efficiency of scattering radiations is obtained. Finally, the appropriate condition to optimize S1 is found.

Key words: atmospheric optics; DIAL; stimulated Raman scattering (SRS)

中图分类号： O431.2 **文献标识码：** A

1 Introduction

Differential absorption lidar (DIAL) is one of effective tools to measure atmospheric pollutants with the highly temporal and spatial resolution, such as NO_2, SO_2 and O_3[1]. Ti:Sapphire and OPO has been operated as laser sources of DIAL. The difficulty is that these tunable laser systems need the precise wavelength control and calibration, and their complexity and expensive maintenance limit their wide application.

Recently, Raman-shifters are used as the UV laser sources for DIAL system because of their stable wavelength shift and simplicity of the setup[2,3]. SRS of H_2, D_2 and CH_4 pumped by fourth harmonic of Nd:YAG has been successfully conducted for O_3-DIAL application[4]. This paper presents the numerical analysis and experiments of SRS of CH_4 pumped by third-harmonic Nd:YAG laser, whose first Stokes (S1) radiation at 395.6 nm may be used as the absorption wavelength of NO_2-DIAL.

2 Experimental setup

The experimental setup of the SRS system, which is used here, is similar to that of Ref.[2]. Nd:YAG laser is in an oscillator-amplifier configuration. The pump light is third-harmonic Nd:YAG laser at 355 nm, with a pulse duration of 18 ns, divergence of 0.5 mrad, maximum pulse energy of 80 mJ, and repetition rate of 10 Hz. Raman cell is made of stainless steel with 1-m long, and it is filled with CH_4 as Raman media with the

Foundation item: supported by Plan-863 National High-technology Research and Development Programme of China.
Received date: 2003-11-26; **Revised date:** 2004-02-12
E-mail: lotusflowers@tom.com

purity 99.99%. Two plane-convex quartz lenses of Raman cell windows have 1.8 cm diameter and focal length 30 cm and 70 cm, respectively, so as to decrease the divergence of output scattering radiation by expanding the beam. A regulable diaphragm is used to change the pump energy and pump beam quality.

Taking the ratio of the two detectors' signals, the absorption and reflection losses at the various optical elements used (Raman cell windows, prism, etc) into account, we get the energy conversion efficiency of the forward SRS effect.

3 Numerical study

In the case of gases, the plane-wave steady-state Raman gain coefficient g_{R1} is given by [3]

$$g_{R1} = \frac{d\sigma}{d\Omega}\frac{2\lambda_s^2 \Delta N}{\pi h c^2 v_i^s \Delta v_R}, \tag{1}$$

where $d\sigma/d\Omega$ is the P-S1 differential Raman cross section (cm^2/sr), h is Plank's constant (J/s), c is the speed of light (cm/s),Δv_R is the Raman linewidth (FWHM in cm^{-1}), λ_s is the Stokes wavelength (cm), ΔN is the population difference between the initial and the final energy levels (cm^{-3}). In case of CH_4[5] $\Delta v_R = 0.32 + 0.122p(cm^{-1})$, where p is the gas pressure (MPa). To achieve the steady-state condition, the pump laser duration T_p should exceed 30 T_2 at least[3], where $T_2 = 1(\pi c \Delta v_R)$ is the dephasing time. Its variation with pressure is shown in Fig.1. It is obvious $T_p \gg 30T_2$ in present experiment, which achieves steady-state conditions.

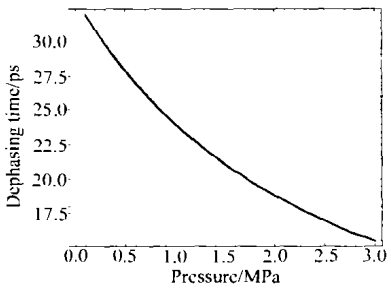

Fig.1 Dephasing times(ps) at different pressure(MPa)

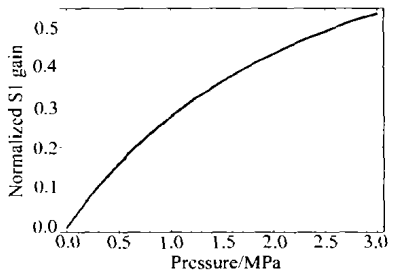

Fig.2 Calculated Raman normalized S1 gain coefficient as a function of gas pressure for CH_4

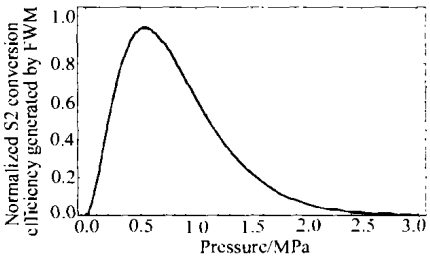

Fig.3 Calculated normalized conversion efficiency of S2 generated only by FWM as a function of gas pressure for CH_4

Assuming that the pump depletion is negligible, the growth of the Stokes field is given [2] : $I_{S1}(l) = I_{S1}(0)e^{g_{p1}lI_p}$, where $I_{S1}(0)$ is the input stokes signal, which arises from the spontaneous Raman scattering and quantum noise, I_p is the intensity of the pump beam, l is the length of the Raman cell, and g_{p1} is the Raman gain coefficient. According to calculation, the normalized Raman gain coefficient of S1, as a function of gas pressure for CH_4, is shown in Fig.2. It can be seen that S1 gain increases persistently with pressure below 3 MPa, so the energy conversion efficiency on S1 increases, too.

When S1 is strong enough, it will generate the second Stokes (S2) by cascade Raman scattering. By neglecting the four-wave mixing (FWM) and other nonlinear processes, the intensity of S2 due to cascade Raman processes is given by the expression

$$I_{S2}(l) = I_{S2}(0)\exp(g_{S2}\int I_p dl). \tag{2}$$

where g_{S2} is the Raman gain coefficient for S2. Similar expressions can be written for the higher-order Stokes radiation.

The high gain leads to Stokes cascade with coexisting FWM processes. FWM is a third-order nonlinear process, and there is no threshold for its creation, but it needs vector phase matching [5]. In general, cascading SRS is the dominant process in a soft focusing geometry. However, in a tight focusing geometry, FWM is the dominant process. If we neglect the higher-order Stokes contribution to S2 and only consider the pump, S1, and first anti-Stokes (AS1), the dominant mixing process in S2 generation would be $\omega_{S2} = 2\omega_{S1} - \omega_{S0}$ because of its smaller wave-vector mismatch. We can conclude that FWM dominates S2 generation at low pressures where the wave-vector mismatch is small; the cascade Raman processes contribute more as the gas pressure is increased and the contribution by FWM decreases.

For a cell whose length is comparable to the laser confocal parameter, assuming that only a lowest-order Gaussian(TEM00) beam is produced, output power P of S2, generated by FWM is given by $P - Bp^2 \exp(-b|\Delta k|)$[6], where B is a constant to be independent of pressure p, b is the laser confocal parameter(cm), and Δk is the wave-vector mismatch caused by the dispersion of the medium. Fig.3 shows theoretical predictions of S2 conversion efficiency for FWM alone in CH_4, normalized to unity at the maximum values. For higher-order Stokes, there are more FWM processes, and those conversion efficiencies are lower in general, which wouldn't be presented here because the analysis is more complicated.

Conversion to anti-Stokes wavelengths from the pump and Stokes proceed only by FWM processes [7]. The anti-Stokes cascading is much more sensitive to the pressure: all the anti-Stokes efficiencies are to decrease with pressure ultimately, due to the increase of wave-vector mismatch, which is different from the Stokes cascading.

4 Experimental result and discussion

By adjusting the regulable diaphragm to select the central part of pump laser beam, pump energy is changed. Scattered-radiations energy percent versus the diameter of diaphragm is shown in Fig.4. Energy percent of S1 increases with the diameter of diaphragm while it is small, and which reaches to maximum 54.78% at diaphragm of 2 mm. Because of lower pump energy, S1 is not strong enough to generate too much S2 as new pump energy. On the other hand, FWM processes are suppressed with smaller aperture. Using the data presented in Ref.[5], we obtain a wave-vector mismatch Δk of 35.67 cm^{-1} for CH_4 at 2.2 Mpa. The phase-match angle [8] given by $\sqrt{k_p \Delta k / k_{S2} k_s}$ is 16.76 mrad. The divergence of the pump beam in the Raman cell is 6.67 mrad with the beam diameter of 2 mm at the entrance window and a focal length of 30 cm. Since the divergence of the pump beam is smaller than the phase-match angle, FWM processes are suppressed. Furthermore, the pump beam is far from diffraction limited[9] ($\theta = 4\lambda/\pi D$, λ=355 nm, D=2 mm, and θ= 0.226 mrad), which also reduces FWM processes. Therefore the higher-order Stokes and anti-Stokes radiations are very weak, and more pump energy is distributed to S1. When the diaphragm is wide enough, the divergence of the pump beam is comparable to the phase-match angle, then the influence of FWM processes are prominent, at the same time, pump energy increases. Both the phase-match and increase of pump energy facilitate the generation of S2, other high-order Stokes and anti-Stokes radiation. In the cascade Raman process, S2 generated can never rise simultaneously with or exceed S1 [6]. It is obvious that S2 exceeds S1 in Fig.4 when diaphragm is larger than 5 mm with pump energy more than 40 mJ, which indicates that a dominant contribution to the generation of S2 comes from FWM. This result accords with analysis above. So, we can use a Raman cell entrance lens with longer focal length, or decrease the divergence of pump beam to suppress FWM for higher energy conversion efficiency on S1.

With a beamsplitter placed in front of the entrance of cell, pump energy decreases to 40 mJ. Without diaphragm, scattered-radiation energy conversion efficiency versus pressure is shown in Fig.5. We find that total energy conversion efficiency (S1+S2+AS1, neglecting other scattered-radiations) is increased with the increase of pressure during the whole course, which reaches the maximum 57.55% at 2.5 MPa. The energy conversion efficiencies of S1 and S2 rise simultaneously with the pressure, and they are almost equal above 1.8 MPa. And the maximum energy conversion efficiency of S1 reaches 28.66% at 2.5 MPa, which is higher than that described in ref.[5]. The changing trend of S1 accords with the analysis in Fig.2. It is found that the energy of stokes radiation is unstable, which drifts about 20% with pump energy variation of less than 10%, and even sometimes S2 is much stronger than S1 for some pulses. The simultaneous increase and intension of S1 and S2 indicate that FWM is prominent for generation of S2. It is easy to know that vector phase matching for the existence of FWM is reached from the calculation according to the formula above. Because of the difference of transverse intensity of the pump beam, the pump energy of the beam edge is less than that described in Fig.4, then S1 is stronger than S2 persistently. From the changing trend of Fig.5, we can say that the measured optimization pressure for S2 is not less than 2.5 Mpa, which is higher than the theoretical predictions in Fig.3. The discrepancy may be due to the interaction of FWM and cascade Raman scattering. Newton and Schindler [10] showed that the ratio of the SRS gain to the FWM phase mismatch was proportionally related to the FWM averaging effect. Another possible reason for the discrepancy is the assumption of a single Gaussian mode, in general, the wave generated by four-wave mixing has a multimode structure which will shift the optimization pressure to the higher side [11].

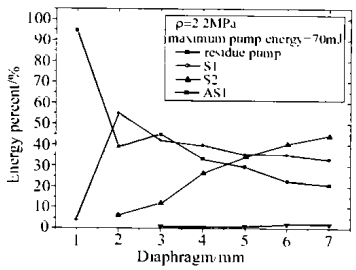

Fig.4 Energy percent(%) on different radiation of the total output energy versus diaphragm(mm).

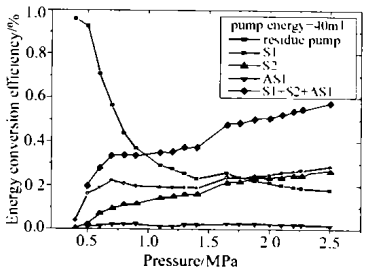

Fig.5 Energy conversion efficiency(%) on different radiation versus pressure(MPA).

The maximum theoretical energy conversion efficiency for a Raman laser is given by $\eta = (v_p - v_R)/v_p$[5] where v_p is the frequency of the third-harmonic of Nd:YAG laser, 8169 cm^{-1}, v_R=2916cm^{-1}, so the maximum energy conversion efficiency is 89.6%. Under the conditions mentioned above, changing pressure of gas, the maximum energy conversion efficiency is 57.55%, which is less than 89.6%. In addition to the Raman forward scattering and FWM processes, there are many loss processes, which may be responsible for the loss of pump energy, such as Raman backward scattering, stimulated Brillouin and Rayleigh scatterings, etc.

5 Conclusion

We have investigated the performance of a single-pass, multi-order stokes generated system using CH_4 as Raman media. It is found that FWM has an important effect on the energy conversion efficiency of S1, which is higher with smaller aperture than that with larger aperture. Given fixed pump energy, the energy conversion efficiencies on S1 and S2 increase with the pressure. Above 1.8 MPa they are almost equal, and the maximum on S1 is 28.66% at 2.5 MPa, at the same time, the energy stability of S1 is better than that at lower

pressure. So we can decrease the divergence of pump beam and increase pressure to optimize S1(395.6 nm) radiation used as λ_{on} for DIAL measurements of NO_2.

Acknowledgements: The authors thank Engineer Qi F D and Dr. Hu S X for their excellent technical assistance, Dr. Tao Z M and Msc Zou J M for helpful discussions and comments on the manuscript.

Referance:

[1] Wu Yonghua, Yue Guming, *et al.* Stimulated Raman scattering pumped by fourth harmonic Nd:YAG laser and its application in laser radar [J]. *Chinese J. Lasers* (中国激光), 2000, A 27: 823-827 (in Chinese).

[2] Xu Ben, Yue Guming, *et al.* Generation of UV laser light by stimulated Raman scattering in D_2, D_2/Ar and D_2/He using a pulsed Nd:YAG laser at 355 nm [J]. *Chin. Phys.*, 2003, 12: 1021-1025.

[3] Schoulepnikoff L, Mitev V, *et al.* Experimental investigation of high-power single-pass Raman shifters in the ultraviolet with Nd:YAG and KrF lasers [J]. Appl. Opt., 1997, 36: 5026-5043.

[4] Haner D A, Mcdermid I S. Stimulated Raman shifting of the Nd:YAG fourth harmonic (266 nm) in H_2, HD, and D_2 [J]. *IEEE J.Quantum Electron.*, 1990, 26: 1292-1298.

[5] Sentrayan K, Major L, *et al.* Observation of intense stokes and anti-Stokes lines in CH_4 pumped by 355nm of a Nd:YAG laser [J]. *Appl. Phys.*, 1992, B55: 311-318.

[6] Chu Zhiping, Upendra N S, Thomas D W. Multiple Stokes wavelength generation in H_2, D_2, and CH_4 for lidar aerosol measurements [J]. *Appl. Opt.*, 1991, 30: 4350-4357.

[7] Schoulepnikoff L, Mitev V. Hihg-gain single-pass stimulated Raman scattering and four-wave mixing in a focused beam geometry: a numerical study [J]. *Pure Appl. Opt.*, 1996, 6: 277-302.

[8] Heuvel J C, Putten F J M, Lerou R J L. Experimental and numerical study of stimulated Raman scattering in an astigmatic focus [J]. *IEEE J. Quantum Electron.*, 1993, 29: 2267-2272.

[9] Lou Qihong. Research on the characteristics of H_2 Raman conversion pumping by a 1-J XeCl excimer laser [J]. *J. Appl. Phys.*, 1989, 66: 2265-2273.

[10] Newton J H, *et al.* Numerical model of multiple-Raman-shifting excimer lasers to the blue-green in H_2 [J]. *Opt. Lett.*, 1981, 6: 125.

[11] Bjorklund G C. Effects of focusing on third-order nonlinear processes in isotropic media [J]. *IEEE J. Quantum Electron.*, 1975, QE-11: 287-296.

CH_4 受激拉曼散射产生紫外激光用于 NO_2 差分吸收激光雷达的研究

徐　贲[1,2]，岳古明[1]，吴永华[1]，周　军[1]，张寅超[1]，胡欢陵[1]

(1 中国科学院安徽光学精密机械研究所大气光学重点实验室，　安徽　合肥　230031；

2 中国计量学院光电子技术研究所，　浙江　杭州　310018)

摘　要：　脉冲 Nd:YAG 三倍频激光 (355 nm) 泵浦 CH_4 的受激拉曼散射第一级斯托克斯光 (395.6 nm) 用作 NO_2 差分吸收激光雷达的 λ_{on}。为研究 CH_4 的受激拉曼散射效应和定量解释其物理机理作了数值模拟计算，并作了一系列的实验。通过调节泵浦能量、光束质量和气体压强，得到了各级散射光的能量转化效率与三者间的函数关系，找到了第一级斯托克斯光的优化条件。

关键词：　大气光学；差分吸收激光雷达；受激拉曼散射

作者简介：　徐　贲　(1979 -)，男，湖北孝感人，1997 年毕业于华中师范大学信息技术系，现在中国科学院安徽光学精密机械研究所大气光学重点实验室攻读硕士，研究方向为大气探测激光雷达用 Nd:YAG 激光器和拉曼激光器等。